JOURNAL OF AIRCRAFT
Vol. 37, No. 5, September–October 2000

Limit Cycle Oscillation Flight Test Results of a Fighter with External Stores

Charles M. Denegri Jr.*
U.S. Air Force SEEK EAGLE Office, Eglin Air Force Base, Florida 32542-6865

Oscillatory wing response data were measured on an F-16A aircraft during flutter tests of several external store configurations. Previous testing had shown the F-16 to exhibit limit cycle oscillations (LCO) in the transonic regime. During the present tests, LCO were encountered as well as the sudden onset of high-amplitude oscillations. This sudden high-amplitude response closely resembled that of classical flutter. In all, three distinct categories of response behavior were seen during these tests: classical flutter, typical LCO, and nontypical LCO. These categories are representative of the broad spectrum of aeroelastic responses encountered by fighter aircraft with external stores. Theoretical flutter analyses are shown to adequately identify flutter- or LCO-sensitive store configurations and their instability oscillation frequencies. In addition, a strong correlation between the flight test response and the modal composition of the analytical flutter mechanism is evident. However, the linear analysis fails to provide insight into the oscillation amplitude or onset velocity, which are of primary importance for external store certification on fighter aircraft. Flutter analysis results are presented along with details of the analytical model, the store configurations, and the store mass properties for use as realistic check cases for the validation of nonlinear flutter analysis methods.

Nomenclature

f_f	=	linear analysis flutter frequency, Hz
f_n	=	natural frequency, Hz
f_t	=	flight-test instability frequency, Hz
$\bar{M}$	=	generalized modal mass, lbf-s^2-in.
M_∞	=	freestream Mach number
V_f	=	linear analysis flutter velocity, knots calibrated airspeed (KCAS)
V_t	=	flight test instability onset velocity, KCAS

Introduction

LIMIT cycle oscillations (LCO) have been a persistent problem on several fighter aircraft and are generally encountered on external store configurations that are theoretically predicted to be flutter sensitive. These sensitivities are quite evident during flight and are often the subject of extensive examination during flutter flight tests of aircraft that exhibit this behavior. Bunton and Denegri[1] provide a detailed description of the LCO phenomenon as well as a discussion of its evolution and its relationship to classical flutter. Norton[2] gives an excellent overview of LCO of fighter aircraft carrying external stores and its sensitivity to the store carriage configuration and mass properties. These articles describe LCO as a phenomenon characterized by sustained periodic oscillations that neither increase nor decrease in amplitude over time for a given flight condition. There is little disagreement in the flutter engineering community that LCO arises from the nonlinear interaction of the structural and aerodynamic forces acting on an aircraft structure. However, there is significant disagreement as to which of these sources is the major contributor to the phenomenon.

Cunningham and Meijer[3] and Meijer and Cunningham[4] have shown that nonlinear aerodynamic forces arising from shock-induced trailing-edge separation are a dominant mechanism in transonic LCO. They investigated several transonic LCO cases and demonstrated success with an analytical approach that uses both steady and unsteady wind-tunnel data for the aerodynamic forces and a linear dynamics model for the structural motions.

Chen et al.[5] approached the problem from a different perspective and assumed that nonlinear structural damping was the significant factor. They presented two aircraft configurations that differed only in the missile launchers carried underwing and on the wingtip. A more refined aerodynamic model of the aircraft and stores was used that led to an improvement in the solution results. Their results showed a humped damping curve with stability transitions that correlated to the onset and subsequent cessation of the LCO measured during flight testing. These results are encouraging for the cases examined. However, their work addressed a category of LCO behavior where the oscillation onset occurs at a relatively low subsonic Mach number. In this case, the linear aerodynamic assumption is quite valid but may not prove quite as useful for the purely transonic cases (such as those presented in the present work).

In this paper, linear flutter analyses will be shown to adequately identify the oscillation frequency and modal composition of the LCO mechanism. However, because of the nonlinearities involved, these classical linear flutter analysis techniques fail to predict the onset or severity of the LCO, which are of prime importance in the certification of external store configurations on fighter aircraft. Some success in predicting LCO has been achieved[3–5] but these approaches have not been demonstrated to adequately predict the wide variety of response characteristics seen in flight. There exists a significant need for an analysis capability that can discern the difference between these types of responses. The flight-test results presented herein are submitted as realistic check cases to aid progress in the development and validation of future analysis codes and methodologies.

Test Aircraft

The aircraft used for this test was an F-16A, tail number 80-0573. This aircraft is a Block 15 F-16 modified for flutter testing. These modifications made it uniquely capable of sensing, recording, and transmitting data gathered during aircraft flutter testing. The F-16 wing is a cropped delta planform blended with the fuselage and is composed of a NACA 64A-204 airfoil with a wingspan of 32 ft, 8 in. The wing aspect ratio is 3.2 and has a leading-edge sweep angle of 40 deg. Extra fuel can be carried in external tanks under the wings and the fuselage and additional stores of various types can be carried on the wingtips, six wing stations, and one fuselage centerline station.

Presented as Paper 2000-1394 at the AIAA/ASME/ASCE/AHS/ASC 41st Structures, Structural Dynamics, and Materials Conference, Atlanta, GA, 3–6 April 2000; received 18 January 1999; revision received 7 April 2000; accepted for publication 29 April 2000.

*Lead Flutter Engineer, Engineering Branch, Certification Division, 205 West D Avenue, Suite 348. Senior Member AIAA.

Data Acquisition, Analysis, and Test Methods

A brief discussion of the data acquisition and analysis process follows. This section serves as an introduction to the test aircraft instrumentation, the flutter excitation system, the test methods, and the data analysis techniques used for the tests presented herein. A complete overview of Eglin Air Force Base flutter testing can be found in Ref. 6.

Test Aircraft Instrumentation

The aircraft flutter and LCO response data were measured using accelerometers located on the forward and aft ends of the wingtip missile launchers. The forward accelerometer was located approximately 4 in. aft of the launcher nose and the aft accelerometer was located approximately 12 in. forward of the launcher tail.[6] The measurement range of these accelerometers was $\pm 10g$ with a nominal sensitivity of 10 mv/g (at 100 Hz) and a noise floor of 0.0012g (rms). Data was acquired at 200 sample/s using a programmable data acquisition system. Control surface position and aircraft flight parameters were also measured.

The test flights were flown over the Eglin Air Force Base water test ranges. The test aircraft transmitted the data via time-correlated signals to the ground receiver station in pulse coded modulation format. Two streams of data were transmitted with the basic aircraft parameters such as Mach number, altitude, and normal g on one stream and the flutter response parameters on the other. The ground receiver station retransmitted the test data to the Central Control Facility where the data were processed for real-time display of selected parameters on strip-chart recorders and video display monitors. Direct air-to-ground communications were available between the aircraft and the control facility to provide test point clearance and to relay test maneuver information.

Flutter Excitation System

A flutter excitation system was installed on the test aircraft and was designed to excite vibration modes in the aircraft structure by introducing an input signal to the flaperon servoactuators, which would move the flaperon a maximum of ± 1 deg at frequencies from 2 to 20 Hz. This system made it possible to excite and identify specific vibration modes at successively higher speeds to accurately determine damping or structural stability at a specific test condition.

The flaperons could be driven in two modes, burst or sweep, by the flutter excitation system. In the burst mode (frequency dwell), the flaperons were deflected for a preselected time period (0.9–5.0 s) at a preselected frequency. In the sweep mode, the excitation frequency of the flaperons was varied continuously starting at 20 Hz and sweeping through the frequencies down to 2 Hz. In each excitation mode, the flaperons could be deflected in the same direction (symmetric) or in opposite directions (antisymmetric). The flutter excitation system was controlled and operated by the flutter excitation control panel that replaced the stores management system panel in the cockpit.

Test Methods

Testing began at 10,000 ft pressure altitude (altimeter set to 29.92 in. Hg) and all test points were generally completed at that altitude before proceeding to another altitude. The onboard excitation system was used to determine the flutter sensitivity at the 10,000- and 5000-ft test points. Elevated load factor turns were also examined to determine the flutter and LCO sensitivity to these maneuvers. A test point maneuver was terminated when the response amplitude either exceeded predetermined termination criteria, or the response amplitude increased at such a rate as to rapidly approach the predetermined termination criteria.

Data Analysis

Time history response was continuously monitored in the control room. The sensitivity to the forced excitation as well as the response decay rate following the excitation was tracked. Frequency domain analysis was used to determine the spectral content (and, hence, the modal composition) of the aircraft response. Approximately 20 s of accelerometer response data were processed with spectral analysis software which yielded a frequency resolution of 0.20 Hz (1024 block size at 200 sample/s). Absolute damping levels were monitored but are not as useful for testing aircraft that routinely encounter LCO. In this case, the aircraft is essentially flown in a condition of neutral stability, that is, zero damping, and the response amplitude and sensitivity to the test maneuvers are examined.

Test Results and Discussion

Results are presented for three external store configurations that exhibited dynamic aeroelastic instabilities during flight testing. In all, three distinct categories of response behavior were seen during the tests and are described as classical flutter, typical LCO, and nontypical LCO. One configuration from each of these categories is presented. The store configurations are listed in Table 1. The store mass properties are presented in Table 2 with the store attachment reference points given in Table 3. The wing response levels for each straight-and-level flight-test point are plotted with respect to Mach number and test altitude. These data are from the forward wingtip launcher accelerometer.

Classical Flutter

Classical flutter behavior is characterized by the sudden onset of high-amplitude wing oscillations. Figure 1 shows flight-test results for the configuration that exhibited classical flutter behavior. At 10,000-ft pressure altitude, the test points from 0.80 to 0.90 Mach progressed smoothly, showing no significant structural responses other than a slightly higher aircraft response to the forced excitation. Residual damping trends following the excitation system frequency dwell (burst) were steady and no sensitivities to the aircraft test maneuvers were evident. At 0.95 Mach, the rapid onset of high-amplitude oscillations was encountered in straight-and-level flight, resulting in termination of the test point. Testing was resumed at 5000 ft, 0.80 Mach. Again, testing progressed smoothly to 0.90 Mach with only a low-level LCO present at this flight condition. This oscillation was stable in level flight but increased rapidly during an elevated load factor turn. Returning to level flight and on accelerating to 0.92 Mach, the rapid onset of diverging oscillations was again encountered. The test point was terminated before the response reached a high level. Similar behavior was seen at the other test altitudes. The instability response was antisymmetric at a frequency of 9.5 Hz for all test points.

Table 1 Store configurations[a]

	Response category		
Station	Classical flutter	Typical LCO	Nontypical LCO
1	LAU-129/A launcher	LAU-129/A launcher	16S210 launcher
2	Empty station[b]	LAU-129/A launcher AIM-9L missile	LAU-129/A launcher AIM-9L missile
3	Launcher/pylon Air–surface missile	Launcher/pylon Air–surface missile	Launcher/pylon AIM-120A missile
4	Empty station[b]	Fuel tank pylon 370-gal fuel tank (empty)	Fuel tank pylon 370-gal fuel tank (empty)

[a]See Table 3 for store station location and type. [b]No store or suspension equipment present.

Table 2 Store mass properties

Store	Weight, lb	Center of gravity[a]			Moments of inertia, slug-ft^2		
		x, in.	y, in.	z, in.	Roll	Pitch	Yaw
Air–surface missile	502.0	−14.58	0.00	−25.00	1.76	139.87	140.00
AIM-9L missile	200.0	−21.10	0.00	−17.50	0.42	51.00	51.00
AIM-120 missile	345.0	−14.73	0.00	−25.00	0.65	96.65	96.59
LAU-129/A wingtip launcher	88.0	−13.72	2.88	0.00	——	13.86	13.86
LAU-129/A underwing launcher	88.0	−13.72	0.00	−14.50	——	13.86	13.86
16S210 wingtip launcher	69.0	−15.28	3.60	0.00	——	11.68	11.68
Launcher/pylon	138.0	−3.60	0.00	−11.20	1.46	14.35	13.55
370-gal fuel tank (empty) plus pylon	438.5	−8.37	0.00	−18.22	17.12	176.11	165.69

[a]Relative to store attachment points, see Table 3.

Table 3 Store attachment reference points

Station	Location	Type	x, in.	y, in.	z, in.
1	Wingtip	Missile	380.46	180.00	0.00
2	Underwing	Missile	375.72	157.00	0.00
3	Underwing	Weapon	349.67	120.00	0.00
4	Underwing	Fuel tank	325.40	71.00	0.00

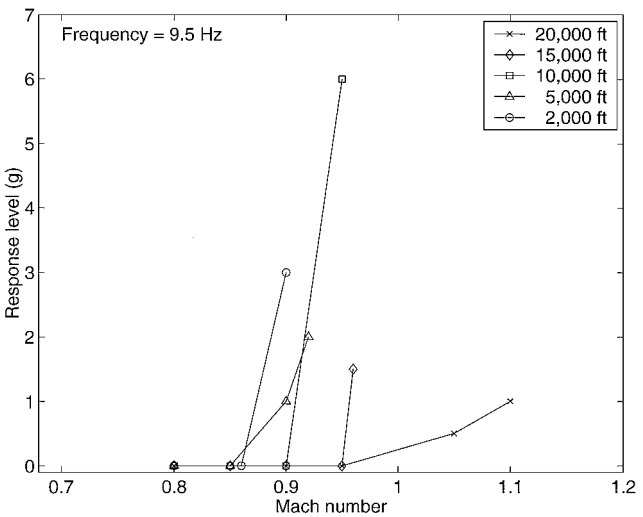

Fig. 1 Measured oscillatory wingtip response during level flight for classical flutter configuration. (Note: Divergent oscillations occurred at all end-points. End-point response levels shown are the maximum measured before test point termination.)

Typical LCO

Typical LCO is characterized by the gradual onset of sustained limited amplitude wing oscillations where the oscillation amplitude progressively increases with increasing Mach number and dynamic pressure. The flight-test results for the typical LCO configuration are shown in Fig. 2. At 10,000 ft, no significant oscillations were present until 0.90 Mach. There, a moderate amplitude LCO was present in level flight and increased slightly during an elevated load factor turn. At 0.95 and 0.96 Mach, the moderate amplitude LCO was present for all test maneuvers. At 5000 ft, low-amplitude LCO was present during a turn at 0.80 Mach and in level flight at 0.85 Mach. At 0.90 Mach, a significant increase in the response amplitude was seen and moderate amplitude LCO was present for all test maneuvers. During level acceleration to 0.91 Mach, an even higher amplitude response was encountered. Level acceleration at 2000 ft showed a progressive increase in LCO amplitudes from no response at 0.75 Mach to a moderate amplitude response at 0.86 Mach. The response behavior of this loading was slightly sensitive to changes in Mach number with increased LCO amplitudes seen for higher Mach numbers. Overall, the dynamic aeroelastic characteristics of this configuration were well behaved. The instability response was antisymmetric at a frequency of 7.8 Hz for all test points.

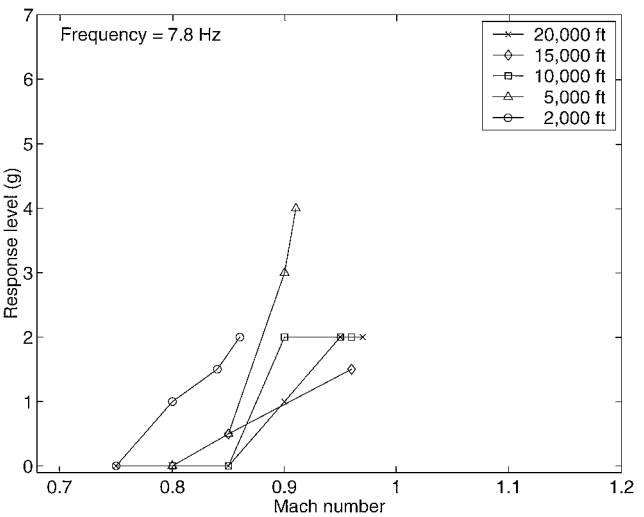

Fig. 2 Measured oscillatory wingtip response during level flight for typical LCO configuration.

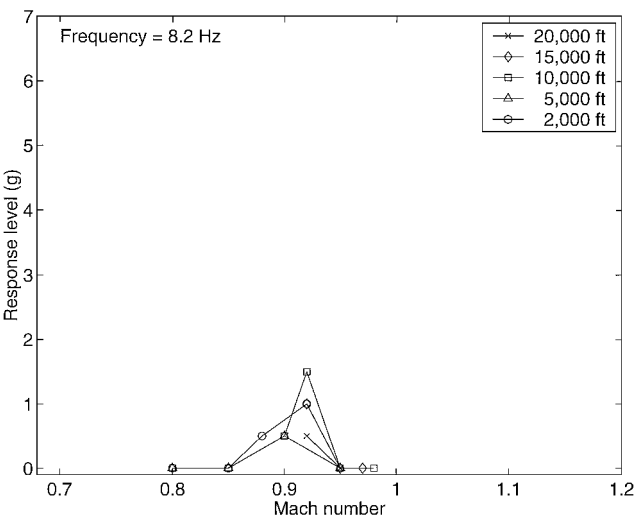

Fig. 3 Measured oscillatory wingtip response during level flight for nontypical LCO configuration.

Nontypical LCO

Nontypical LCO is characterized by the gradual onset of sustained limited amplitude wing oscillations where the oscillation amplitude does not progressively increase with increasing Mach number. Oscillations may be present only in a limited portion of the flight envelope. The flight-test results for the nontypical LCO configuration are shown in Fig. 3. At 10,000 ft, no oscillations were present until at 0.90 Mach, where low amplitude LCO was present during all test events. These oscillations increased slightly at 0.92 Mach during level acceleration, then ceased above 0.92 Mach. At 5000 ft,

low amplitude LCO was present during a dive to 0.90 Mach and increased slightly during a turn. At 0.95 Mach, low amplitude LCO was present during a turn but not in level flight. At 2000 ft, low amplitude LCO was present at 0.88 Mach and increased slightly at 0.92 Mach. Similar response behavior was seen at the 15,000- and 20,000-ft test altitudes. The response behavior of this configuration was only sensitive in the 0.88–0.94 Mach range. For all test altitudes no LCO was present above 0.94 Mach. The instability response was antisymmetric at a frequency of 8.2 Hz for all test points.

Antisymmetric vs Symmetric LCO

All of the cases presented in this paper exhibit antisymmetric LCO. In fact, LCO seems to be predominantly an antisymmetric phenomenon. Symmetric LCO has been encountered, however, not anywhere nearly as often as antisymmetric LCO. It may be possible to explain this tendency toward antisymmetric LCO by considering whether side-to-side energy transfer between flexible wing modes can perpetuate or inhibit LCO. To examine this hypothesis, consider the antisymmetric and symmetric modes that involve predominantly outboard wing motion or inboard wing motion.

Antisymmetric, Outboard Wing Motion

The modal motion of an aircraft wing can be generally described as either bending or twisting in nature. For antisymmetric motion of the outboard part of the wing, bending and twisting modes would impart primarily a rolling moment to the fuselage due to the change in lift at the wingtips. These rolling moments would not be impeded by any aircraft structure and would only be minimally impeded by the aerodynamic forces acting on the fuselage. Because the resulting rolling motion would occur at the same frequency as the wing vibration, this would result in an energy transfer path through the aircraft structure. The frequency response and inertia characteristics of the opposite wing would interact with this energy transfer and perpetuate the vibratory motion.

Symmetric, Outboard Wing Motion

For symmetric motion of the outboard part of the wing, bending and twisting modes would impart a pitch or plunge to the fuselage, but these motions would probably not be very large due to the minimal wing root motion of these types of modes. These types of motion would be heavily resisted by the aerodynamic forces acting on the fuselage and tail surfaces. Consequently, these modes would not contribute much energy to the opposite wing and, thus, would inhibit any oscillatory motion.

Antisymmetric, Inboard Wing Motion

Antisymmetric modes that impart a twisting component near the wing root would encounter significant resistance to side-to-side energy transfer due to the stiffness of the fuselage structure. Bending modes that induce a plunging motion at the wing root would impart a roll component to the fuselage, with accompanying effects as for the antisymmetric, outboard wing motion case, that is, no structural resistance and minimal aerodynamic resistance to the side-to-side energy transfer that would perpetuate the oscillatory motion.

Symmetric, Inboard Wing Motion

Symmetric bending and twisting motions near the wing root would not be impeded by any physical structure and would impart plunge or pitch components to the fuselage. These fuselage oscillations would likely be larger in amplitude than for the symmetric, outboard wing motion case and could be large enough to overcome the fuselage aerodynamic forces. Thus, side-to-side energy transfer would occur and perpetuate any oscillatory motion.

Conclusion

In subsequent sections it will be seen that the free vibration modes that make up the predicted flutter (and, thereby, LCO) mechanism for the cases presented here show the largest deflections at the wing tip. These modes are antisymmetric and the resulting motion at the wingtips has both bending and twisting components with little, if any flexible motion at the wing root. From the preceding discussion, it is apparent that these modes would impart a rolling moment to the aircraft fuselage, thus establishing an energy transfer path for antisymmetric LCO.

Furthermore, the preceding discussion suggests that all antisymmetric modes (those with both inboard and outboard wing motion) have an energy transfer path through the aircraft structure due to the associated wing root roll components. In contrast, the structural energy transfer path of symmetric, outboard wing motion modes is inhibited by the aerodynamic forces acting on the fuselage and tails. It is readily apparent that symmetric modes only have an energy transfer path when the wing root deflections overcome the fuselage aerodynamic resistance to pitch or plunge motions. Therefore, because antisymmetric modes create more viable side-to-side energy transfer paths than do symmetric modes, one would expect to encounter antisymmetric LCO more often than symmetric LCO. The foregoing offers a plausible explanation for the predominant antisymmetric behavior of LCO.

Observations from Linear Flutter Analyses

Linear flutter analyses are accomplished for each configuration to highlight the strengths and inadequacies of using these methods for predicting the types of response seen during the flight tests. The linear flutter analysis results are presented for each store configuration and are discussed in the following. Note that these analyses are not matched analyses but merely worst-case screening analyses.

The flutter analysis model is shown in Fig. 4. The aerodynamic model is a doublet-lattice method[7] representation composed of five panels (fuselage, inner wing, flaperon, outer wing, and wingtip launcher) that are subdivided into 170 discrete boxes. No aerodynamic modeling of the underwing stores is included. The only influence of the underwing stores considered in the flutter analyses is their effect on the structural modal characteristics, that is, mode shapes and frequencies. The aircraft structure is represented by a lumped mass model derived from a finite element model. It is composed of 133 flexibility influence coefficient points for the basic aircraft (wing, fuselage, and empennage) with up to an additional 34 flexibility influence coefficients for the underwing stores, pylons, and launchers. By considering only the modal deflections that influence the aerodynamic model, the system reduces to 75 structural points. The free vibration analyses are performed for a half-airplane model using a matrix iteration method. Aerodynamic influence coefficients are computed for a range of reduced frequencies using sea-level density and 0.90 Mach. The aerodynamic panels are splined to the vibration modes using the method of Harder and Desmarais.[8] The flutter equations are solved using the Laguerre iteration method (see Ref. 9), which is a variation of the classical k method of flutter determinant solution. The first 16 antisymmetric flexible modes were retained for the initial flutter analyses. These modes included all fundamental wing modes and several store modes. A modal deletion study was then accomplished to isolate the primary modes in the predicted instability mechanism. Only these primary mechanism modes are discussed in the following and included in Figs. 5–14. Symmetric modes were not considered in the analyses because it was known from the flight-test results that the actual instability was antisymmetric.

For the flutter analysis results discussed in the following, a critical point is considered to be the velocity at which a modal stability curve crosses from stable (negative structural damping required to produce neutral stability) to unstable (positive) damping. The analytical flutter speed is the critical point associated with the known aeroelastically sensitive mode for the particular configuration. For comparison purposes, the analytical flutter speed is considered to be directly comparable to the lowest airspeed at which self-sustained oscillations are encountered in flight. These oscillations could be either LCO or flutter. The velocity sensitivity of a mode is indicated by the slope of the modal damping curve. Steep slopes indicate rapid decreases in stabilizing damping with increased velocity.

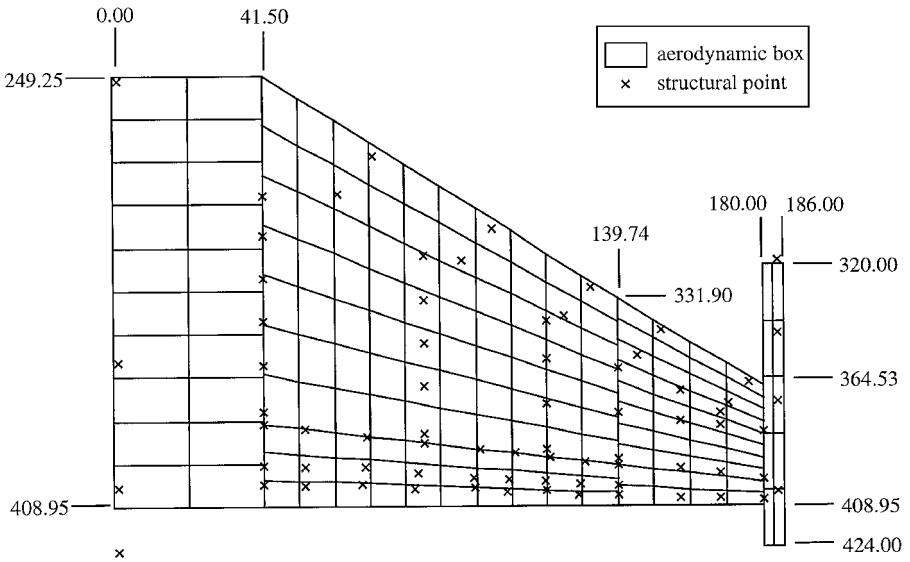

Fig. 4 Flutter analysis model composed of doublet-lattice aerodynamics and lumped mass structure (all dimensions in inches).

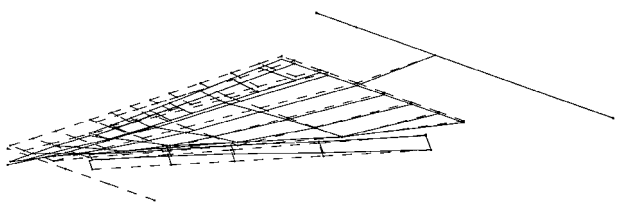

Fig. 5 Classical flutter forward wing torsion mode: f_n = 10.246 Hz and $\hat{M}$ = 1.000 lbf-s^2-in.

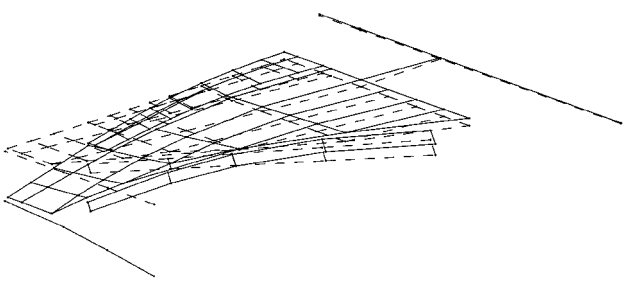

Fig. 6 Classical flutter bending mode: f_n = 9.191 Hz and $\hat{M}$ = 1.000 lbf-s^2-in.

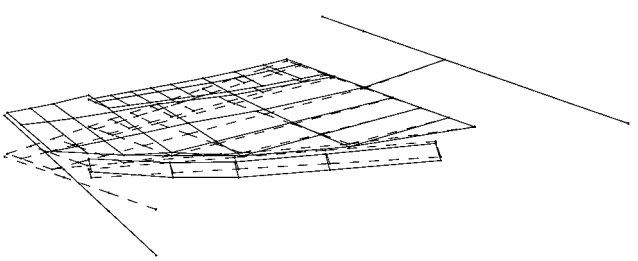

Fig. 7 Classical flutter torsion mode: f_n = 9.964 Hz and $\hat{M}$ = 1.000 lbf-s^2-in.

It is seen for each of the three response categories that a particular set of modes are present in the linear analysis flutter mechanism. Reference 10 showed a distinct correlation between flutter and LCO behavior and the free vibration wing modes composing the linear analysis flutter mechanism. Essentially, it was shown that different linear analysis flutter mechanisms correlated to different aeroelastic responses in flight. To this end, the mode shapes of the critical modes are presented in three-dimensional perspective with the structural points interconnected to outline the wing shape. This provides for easy visual identification of the wing deformation and facilitates use of the modes in flutter analysis codes. The frequencies and generalized masses of these critical modes are also included.

Classical Flutter

Flutter analyses for the classical flutter configuration show two critical points of interest (Fig. 4). The first occurs at 428 kn calibrated airspeed (KCAS) at 10.17 Hz for the forward wing torsion mode (Fig. 5). The node line for this mode is parallel to the leading edge and extends from midchord at the wingtip to the leading edge at the wing root. The damping curve for this mode shows a hump with a shallow slope crossing the 1% structural damping level at 845 KCAS. The second critical point is the flutter sensitive mode for this configuration. The analyses show the first wing bending mode (Fig. 6) goes unstable at a speed of 669 KCAS at 9.35 Hz and is slightly coupled with the first torsion mode (Fig. 7). The node line for the bending mode is oriented chordwise with a slight curve outboard at the leading edge. It extends from midspan at the leading edge to midspan at the trailing edge. The node line for the torsion mode is perpendicular to the fuselage and extends from forward of midchord at the wing root to midchord of the wingtip launcher. The damping curve for the flutter mode shows a steep slope reaching the 1% damping level at 726 KCAS. The flutter analyses indicate a strong sensitivity of the flutter mode to velocity changes and, thus, show good correlation to the flight-test response data as well as the flight-test frequency of 9.5 Hz. However, the analysis results for the flutter mode show a significantly higher instability speed than that seen in flight. The modal deletion study showed the low damped forward wing torsion mode to be an important component of the flutter analysis mechanism. Because of the proximity of this mode's frequency to that of the actual instability, it was not possible to confirm its influence during the flight test.

Typical LCO

Flutter analyses for the typical LCO configuration (Fig. 8) show a flutter speed of 308 KCAS at 8.09 Hz for the forward wing bending mode (Fig. 9), which is coupled with the aft wing bending mode (Fig. 10). The forward wing bending mode shows the largest deflection at the outboard forward part of the wing. Its node line extends from midspan at the leading edge to the wingtip at the trailing edge. The aft wing bending mode shows the largest deflection at the outboard aft part of the wing. Its node line extends from the trailing edge at the wing root to outboard of midspan at the leading edge, curving through the wingtip launcher. Note that each of these modes possesses both bending and torsion components and that pure bending and torsion modes were not present in the vibration solution results. The damping curve for the flutter mode shows a shallow

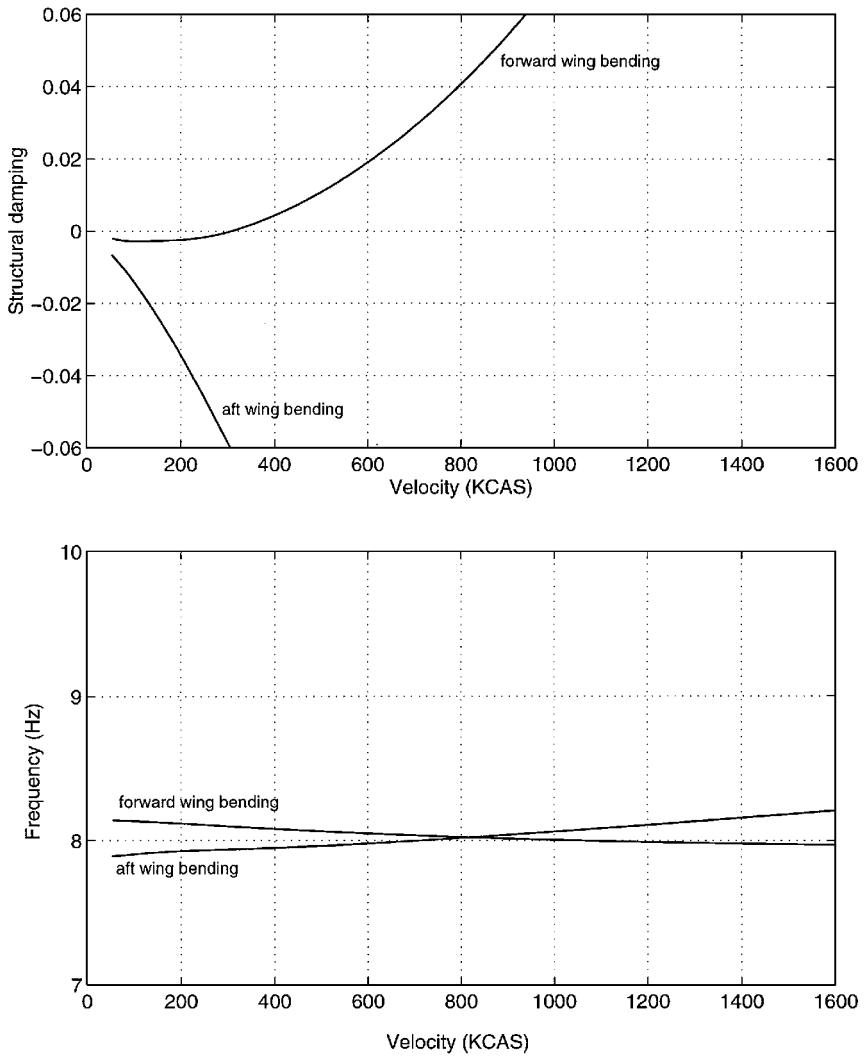

Fig. 8 Flutter analyses for typical LCO configuration: M_∞ = 0.90, sea level, V_f = 308.4 KCAS, and f_f = 8.09 Hz.

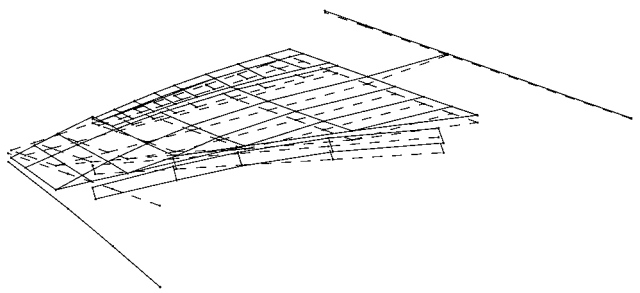

Fig. 9 Typical LCO forward wing bending mode: f_n = 8.149 Hz and $\hat{M}$ = 1.000 lbf-s^2-in.

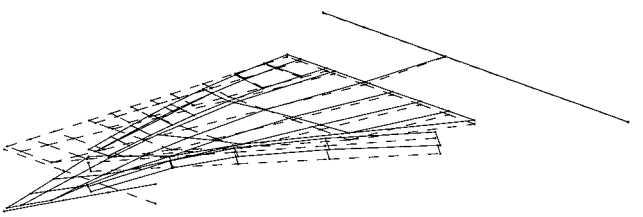

Fig. 10 Typical LCO aft wing bending mode: f_n = 7.891 Hz and $\hat{M}$ = 1.000 lbf-s^2-in.

slope and crosses the 1% damping level at 489 KCAS. A second critical point of 741 KCAS at 10.06 Hz for the wingtip launcher pitch mode was evident in the initial analyses. The damping curve for this mode showed essentially a zero slope and remained in the immediate vicinity of zero damping, showing no tendency toward going more unstable. Modal deletion studies showed this mode to have no effect on the predicted flutter speed. The flutter analyses indicate the flutter critical mode to be slightly sensitive to changes in airspeed and, thus, show good correlation to the flight-test data for velocity sensitivity. In addition, the flutter analysis shows good correlation to the flight-test frequency of 7.8 Hz but is approximately 200 kn conservative with respect to the oscillation onset speed. The wingtip launcher pitch mode was not evident during the flight test.

Nontypical LCO

Flutter analyses for the nontypical LCO configuration (Fig. 11) show a flutter speed of 392 KCAS at 8.25 Hz for the forward wing torsion mode (Fig. 13) coupled with the first wing bending mode (Fig. 14). The forward wing torsion mode for this case is very similar to the classical flutter forward wing torsion mode (Fig. 5). The node line is parallel to the leading edge and extends from the leading edge at the wingtip to the leading edge at the wing root. The bending mode for this case is also very similar to the classical flutter bending mode (Fig. 6). The node line for this mode is oriented chordwise with a slight curve outboard at the leading edge. It extends

Table 4 Summary

Configuration	Vibration analysis Mode	f_n	Flutter analysis V_f	f_f	Flight test V_t^a	f_t
Classical flutter	Forward wing torsion	10.246	428.4	10.17	——	——
	Wing bending	9.191	669.5	9.35	585	9.5
	Torsion	9.964	——	——	——	——
Typical LCO	Forward wing bending	8.149	308.4	8.09	530	7.8
	Aft wing bending	7.891	——	——	——	——
Nontypical LCO	Forward wing torsion	8.313	392.5	8.25	560	8.2
	Wing bending	8.284	——	——	——	——

[a]Oscillation onset velocity for all test altitudes extrapolated to sea level.

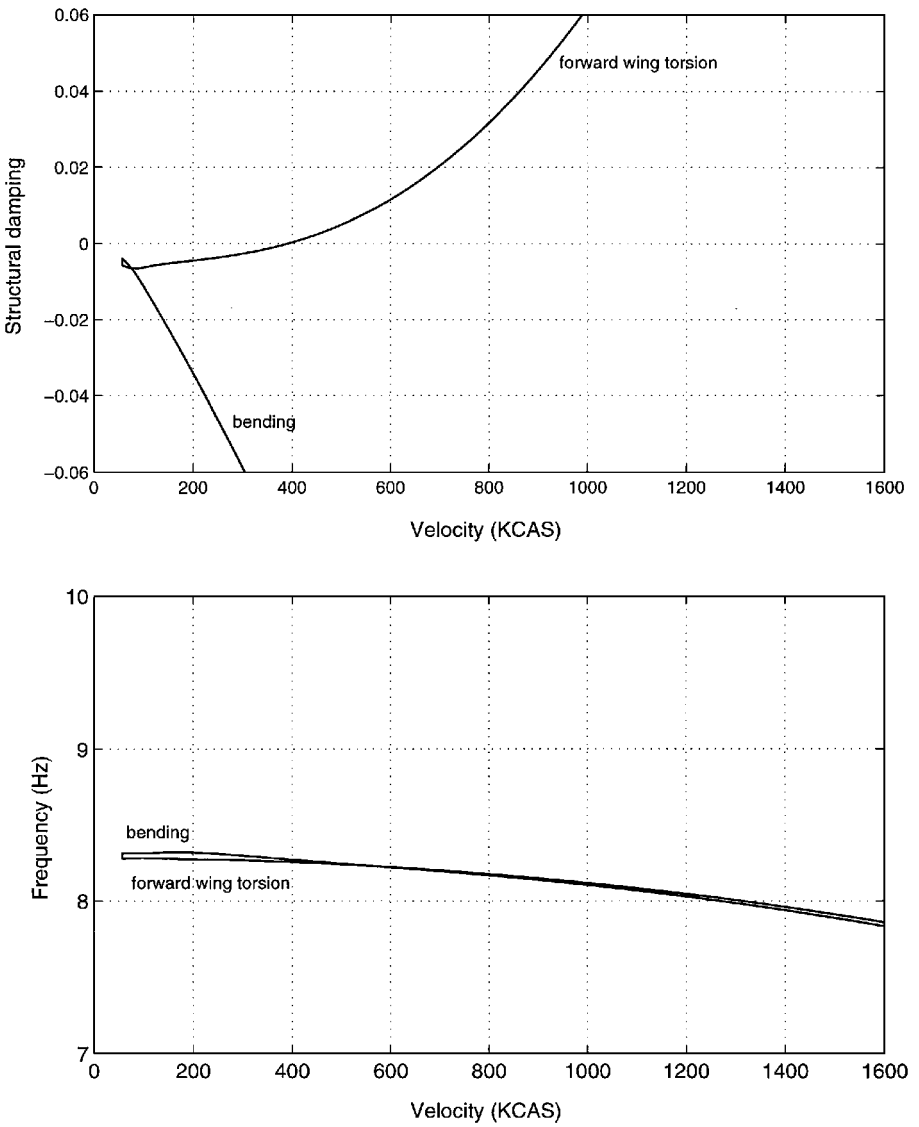

Fig. 11 Flutter analyses for nontypical LCO configuration: $M_\infty = 0.90$, sea level, $V_f = 392.5$ KCAS, and $f_f = 8.25$ Hz.

from midspan at the leading edge to midspan at the trailing edge. The primary difference between the linear flutter analysis results for these configurations is that, for the nontypical LCO case, the forward wing torsion mode is coupled with the first wing bending mode. The flutter analyses for the nontypical LCO case show that the free vibration frequencies of the primary mechanism modes are very close, with the bending mode slightly lower than the forward wing torsion mode. The frequency vs velocity plot shows that the bending mode frequency increases once aerodynamics are applied and becomes greater than the forward wing torsion mode frequency. This tendency remains until the modes couple near 400 KCAS. The damping curve for the flutter mode shows a shallow slope and reaches the 1% damping level at 579 KCAS. The flutter analysis indicates a very slight sensitivity to velocity changes but does not indicate that the oscillations will subside at higher velocities. Thus, the flutter analyses show good correlation to the flight-test data for instability onset speed, but poor correlation for velocity sensitivity. Excellent correlation to the flight-test oscillation frequency of 8.2 Hz is seen.

Table 4 provides a summary of the flutter analysis and flight test results for all configurations. For purposes of comparison to the flutter analyses, the flight test onset velocity is roughly approximated

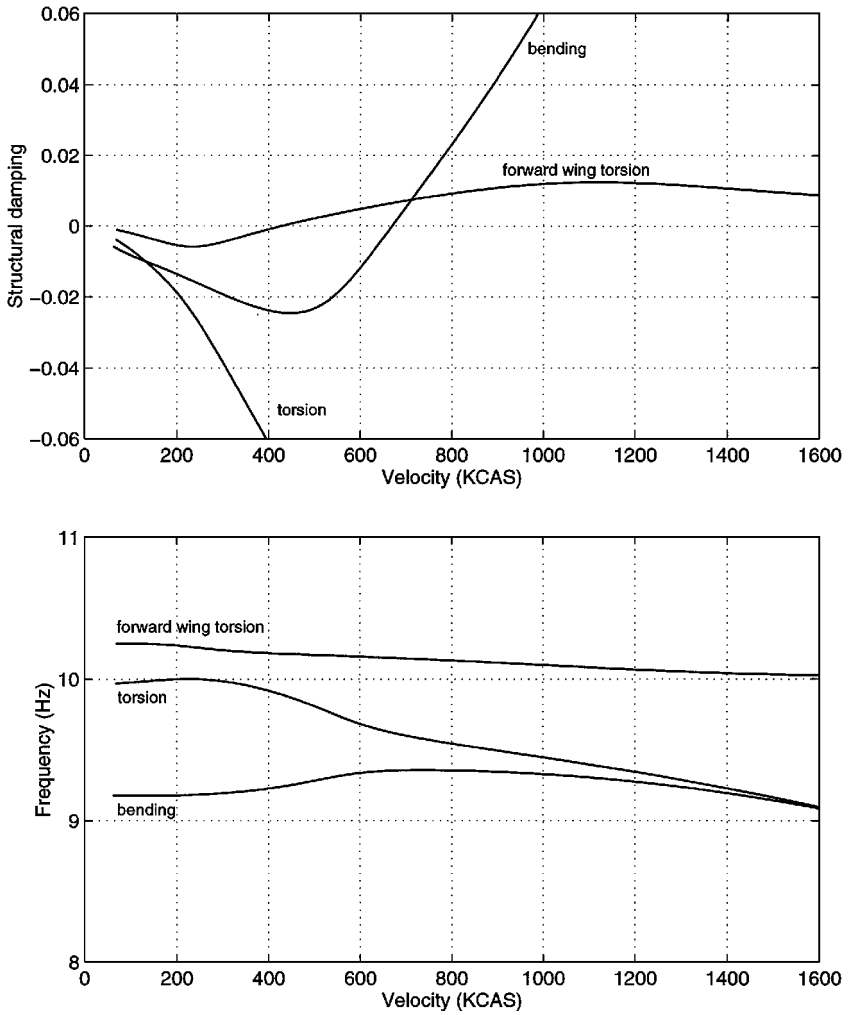

Fig. 12 Flutter analyses for classical flutter configuration: M_∞ = 0.90, sea level, $V_{f,1}$ = 428.4 KCAS, $f_{f,1}$ = 10.17 Hz, $V_{f,2}$ = 669.5 KCAS, and $f_{f,2}$ = 9.35 Hz.

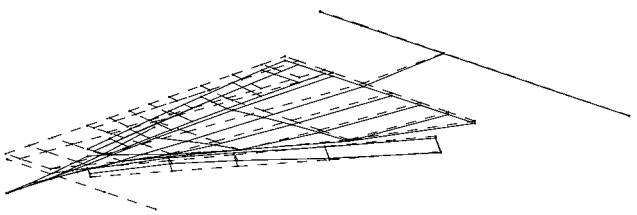

Fig. 13 Nontypical LCO forward wing torsion mode: f_n = 8.313 Hz and $\hat{M}$ = 1.000 lbf-s^2-in.

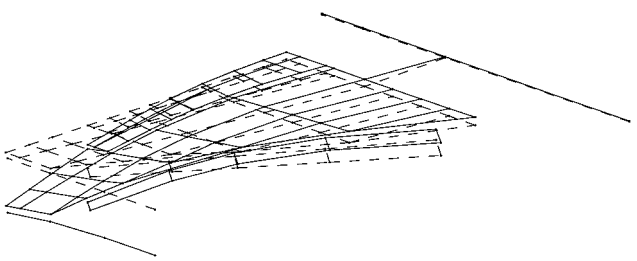

Fig. 14 Nontypical LCO bending mode: f_n = 8.284 Hz and $\hat{M}$ = 1.000 lbf-s^2-in.

by extrapolating to sea level the velocities of the oscillation onset at each test altitude.

Conclusions

Oscillatory wing response data were measured on an F-16A aircraft during flutter testing of several external store configurations. In previous tests with this type of aircraft, LCO were encountered in the transonic flight regime. During the present tests, LCO were again encountered, as well as an apparent classical flutter response. In all, three distinct aeroelastic response types were seen during these tests and were categorized as classical flutter, typical LCO, and nontypical LCO. These categories are representative of the wide variety of aeroelastic responses encountered by fighter aircraft with external stores.

Details of a linear flutter analysis model were presented that included the structural and aerodynamic models, the free vibration mode shapes, natural frequencies, and generalized masses, and the linear flutter analysis velocity vs frequency and damping results. The flight-test results were presented showing the envelope and oscillation frequency of the instability.

The theoretical linear flutter analyses are shown to adequately identify the instability oscillation frequencies and also show a strong correlation between the flight-test response behavior and the modal composition of the analysis flutter mechanism. However, the linear analysis fails to provide insight into the oscillation amplitude or the oscillation onset velocity. These parameters are of primary importance for external store certification on fighter aircraft. Thus,

although linear flutter analyses are useful, they are rather limited in providing sufficient information for certification, and extensive flight testing is required to adequately define a safe, useable flight envelope.

To alleviate the need for extensive flight testing, a nonlinear flutter analysis methodology is required that is capable of discerning between the types of responses presented in this paper. The test results presented herein represent a variety of response characteristics that must be adequately predicted by nonlinear flutter analysis codes. These realistic check cases are presented to further aid progress in the development and validation of these analysis codes.

References

[1]Bunton, R. W., and Denegri, C. M., Jr., "Limit Cycle Oscillation Characteristics of Fighter Aircraft," *Journal of Aircraft*, Vol. 37, No. 5, 2000, pp. 916–918.

[2]Norton, W. J., "Limit Cycle Oscillation and Flight Flutter Testing," *Proceedings of the 21st Annual Symposium*, Society of Flight Test Engineers, Lancaster, CA, 1990, pp. 3.4-1–3.4-12.

[3]Cunningham, A. M., Jr., and Meijer, J. J., "Semi-Empirical Unsteady Aerodynamics for Modeling Aircraft Limit Cycle Oscillations and Other Non-Linear Aeroelastic Problems," *Proceedings of the International Forum on Aeroelasticity and Structural Dynamics*, Royal Aeronautical Society, London, Vol. 2, 1995, pp. 74.1–74.14.

[4]Meijer, J. J., and Cunningham, A. M., Jr., "Semi-Empirical Unsteady Nonlinear Aerodynamic Model to Predict Transonic LCO Characteristics of Fighter Aircraft," AIAA Paper 95-1340, April 1995.

[5]Chen, P. C., Sarhaddi, D., and Liu, D. D., "Limit-Cycle Oscillation Studies of a Fighter with External Stores," AIAA Paper 98-1727, April 1998.

[6]Dreyer, C. A., and Shoch, D. L., "F-16 Flutter Testing at Eglin Air Force Base," AIAA Paper 86-9819, April 1986.

[7]Albano, E., and Rodden, W. P., "Doublet-Lattice Method for Calculating Lift Distributions on Oscillating Surfaces in Subsonic Flows," *AIAA Journal*, Vol. 7, No. 2, 1969, pp. 279–285.

[8]Harder, R. L., and Desmarais, R. N., "Interpolation Using Surface Splines," *Journal of Aircraft*, Vol. 9, No. 2, 1972, pp. 189–191.

[9]Desmarais, R. N., and Bennett, R. M., "Automated Procedure for Computing Flutter Eigenvalues," *Journal of Aircraft*, Vol. 11, No. 2, 1974, pp. 75–80.

[10]Denegri, C. M., Jr., and Cutchins, M. A., "Evaluation of Classical Flutter Analyses for the Prediction of Limit Cycle Oscillations," AIAA Paper 97-1021, April 1997.